The effect of electric fields on the rupture of thin viscous films by van der Waals forces

K. Savettaseranee[1], D. T. Papageorgiou[1], P. G. Petropoulos[1], B. S. Tilley[2]

[1] Department of Mathematical Sciences and
Center for Applied Mathematics and Statistics
New Jersey Institute of Technology, Newark, NJ 07102

[2] Franklin W. Olin College of Engineering
Needham, MA 02492

CAMS Report 0203-06, Fall 2002

Center for Applied Mathematics and Statistics

NJIT

The effect of electric fields on the rupture of thin viscous films by van der Waals forces

K. Savettaseranee, D. T. Papageorgiou*, P. G. Petropoulos, and B. S. Tilley†
Department of Mathematical Sciences and
Center for Applied Mathematics and Statistics
New Jersey Institute of Technology
University Heights
Newark, NJ 07102

We examine the stability of a thin two-dimensional incompressible liquid film when an electric field is applied in a direction parallel to the initially flat bounding fluid interfaces, and study the competition between surface tension, van der Waals, viscous and electrically induced forces. The film is assumed to be sufficiently thin, and the surface tension and electrically induced forces are large enough that gravity can be ignored to the leading order. We analyze the nonlinear stability of the flow by deriving and numerically solving a set of nonlinear evolution equations for the local film thickness and the horizontal velocity. We find that the electric field forces enhance the stability of the flow and can remove rupture. If rupture occurs then the form of the singularity, to leading order, is that found in the absence of an electric field.

* Author to whom correspondence should be addressed.
† Present address: Franklin W. Olin College of Engineering, 1795 Great Plain Avenue, Needham, MA 02492-1245.

I. INTRODUCTION

Macroscopic thin liquid films are important in a variety of applications from biophysics and engineering. One of the important and central phenomena in the dynamics of thin films, is the phenomenon of rupture. Many physical processes involve rupture phenomena and more specifically that of free liquid films. For example, instability and rupture of such films can be found in colloid and bicolloid systems and particlar applications involve the rupture of soap films, coalescence of emulsions, fusion of lipid bilayers or biological membranes, to mention a few (see for example Prevost and Gallez[1,2] and references therein). In engineering applications, thin films are explored in heat and mass transfer process to limit fluxes and to protect surfaces in extreme operating conditions.

A liquid layer on a planar solid boundary is unstable when the layer is ultrathin ($100-1000$ Å). The instability occurs due to long-range van der Waals molecular forces which can cause rupture of the layer. Deryagin[3] first recognized that an excess pressure can be found in a thin liquid layer compared with the pressure in the bulk phase - he termed this excess pressure the "disjoining pressure". A negative disjoining pressure is found in films with higher pressure than that of the bulk phases as when van der Waals forces act between bodies whose characteristic dimensions are large compared to interatomic distance; in this case thinning occurs leading to rupture. In the presence of electric double-layer potentials, a stabilizing competition is set up due to the positive disjoining pressure of the new effect. This can then lead to what are called black films as described by Overbeek[4].

Vrij[5] examined the problem of finding the thickness at which a nondraining film became unstable because of van der Waals forces. A static stability analysis is used to calculate a marginally stable thickness at which small disturbance first start to grow. Ruckenstein and Jain[6] consider a more general stability theory for a film on a horizontal plate. The theory was based on the Navier-Stokes equations modified by the van der Waals forces. They find that the most unstable wave has a wavelength which is large compared to the film thickness. The linear stability of radially bounded thinning free films for which the base state is time dependent (and calculated by lubrication theory) was investigated by Gumerman and Homsy[7]. The nonlinear problem of a liquid film on a solid substrate was addressed by Williams and Davis[8], who used long wave asymptotics to derive a nonlinear partial differential equation capable of describing large amplitude disturbances (the disturbances scale with the film thickness but are long compared to it). The evolution equation retains the effects of surface tension, viscous and van der Waals forces. The equation was solved numerically by Burelbach, Bankoff and Davis[9], who examined the structures near rupture. Much more accurate numerical solutions capable of resolving the singularity structure, have been carried out by Zhang and Lister[10], who also propose similarity solutions for the singularity. The

stability of such similarity solutions is considered by Witelski and Bernoff[11].

Work on the linear stability of a free film has been carried out by Ruckenstein and Jain[6]. Prevost and Gallez[1,2] attempted to derive a nonlinear evolution equation by using long wave theories and managed to do so for relatively large values of surface viscosity; this leads to a single nonlinear partial differential equation for the interface and the effects of surface tension and van der Waals forces are included. Sharma and Ruckenstein[12] studied this case as well and got a valid nonlinear evolution equation for the interface shape. A more general situation is described by the work of Erneux and Davis[13], who derive a coupled set of evolution equations starting from the Navier-Stokes equations. Numerical solutions of these equations are considered by Ida and Miksis in a series of articles[14],[15],[16]. A comprehensive review of the subject of the stability of thin films can be found in Oron, Davis, and Bankoff[17]. A recent numerical study of the Erneux and Davis evolution equations has been carried out by Vaynblat, Lister and Witelki[18], who use adaptive grids to integrate accurately to times very close to the singularity and are thus able to resolve the structure in a definitive way. It is found that at rupture the main balances are between inertia, viscosity and van der Waals forces, with surface tension forces negligible. This leads to similarity solutions of the first kind as opposed to those of the second kind proposed by Ida and Miksis. Our work is consistent with the findings of Vaynblat et al.[18].

When electric fields are present there are additional physical effects including body forces due to currents in conducting fluids, and Maxwell stresses at free interfaces. Melcher and Schwarz[19] examined the effect of an electric field on the linear stability of a sharp interface separating two non-conducting dielectric fluids of infinite extent. A constant electric field was applied in the plane of the undisturbed interface and they investigated the linear stability of viscous and inviscid fluid in the absence of van der Waals forces. El-Sayed[20] considered the linear stability of an electrified fluid sheet when aerodynamic effects in the surrounding medium are important and found that the field stabilizes the flow. Wendel, Gallez and Bisch[21], consider the stability of a dielectric film in the presence of double layer potentials. The potential and charge distributions in the film are taken as given, and two cases are studied: a linear potential drop across the film and no charge on the interfaces, and, finite surface charge on the interfaces and zero potential drop across the film. A linear stability analysis is carried out in the presence of van der Waals forces, which shows that the surface charge induces oppositely charged double layers that enhance the van der Waals instability.

In the case of perfectly conducting viscous fluids, a normal electric field can destabilize the interface. Gonzalez and Castellanos[22], studied the nonlinear stability of perfectly conducting film flow down an inclined plane, and derived a nonlinear evolution equation which includes a Hilbert transform type term due to the electric field. A weakly nonlinear version of this equation provides a modification of the Kuramoto-Sivashinsky equation with the electric

field acting to add or remove active modes to the system. Qualitative features are given, but a careful numerical study has not been carried out.

Tilley, Petropoulos and Papageorgiou[23] investigated the stability of a thin two dimensional liquid film when a uniform electric field was applied in a direction parallel to the initially bounding interface and examined the distinct physical effect of surface tension and electrically induced force for an inviscid, incompressible non-conducting fluid. They analyzed the nonlinear stability of the flow by deriving a set of evolution equations for the local film thickness and local horizontal velocity. Periodic traveling waves were examined and their behavior was studied as the electric field was increased. A modulational instability of the wave trains was also found in both the absence and presence of an electric field, and it was shown that very low level but long perturbations can lead to film rupture. They carried out extensive simulations of the initial value problem that showed that the presence of the electric field caused a nonlinear stabilization.

In the present work we derive a system of nonlinear evolution equations that goven the stability of free films in the presence of a horizontal electric field. The electric field effects appear as a non-local term proportional to the Hilbert transform of the leading order interfacial curvature. We are able to study the competing effects of inertia, van der Waals forces, surface tension and electric fields. This is done computationally by use of accurate pseudo-spectral techniques.

II. GOVERNING EQUATIONS

A thin horizontal liquid layer of undisturbed dimensional thickness $2d$, is bounded by two vertical electrodes a distance $2L$ apart having a constant voltage difference V_0 between them. The constant voltage difference implies a static situation and consequently magnetic effects can be neglected; since electric and magnetic phenomena decouple the appropriate equations to be addressed are Laplace's equation for the voltage potential. As the fluid interface deforms and sets up a time dependent motion, the above assumptions are valid because the time-scale of induced charge re-distribution on the interface, is instantaneous compared to the fluid time-scale.

In the undisturbed state the liquid layer has uniform thickness and the voltage potential difference drives a horizontal electric field, which is different in the liquid and the surrounding medium due to differences in the respective permitivities. We assume further that the fluid is non-conducting and that there is no free charge in the system initially. The former condition in turn implies that there will be no forces due to the field in the liquid region (such effects could be accounted for by body forces in the Navier-Stokes equations), and the latter implies that the system will remain charge-free at later times also, since no sources

are present. In the present setup, then, the electric field is felt through the Maxwell stresses which supplement the viscous stresses in the normal stress balance boundary condition.

The liquid layer is assumed to be sufficiently thin that van der Waals forces are effective. The liquid is a Newtonian viscous fluid having viscosity μ and constant density ρ. Gravity is neglected in this study, an assumption which is valid if the Bond number - the ratio of gravitational to capillary forces - is small. We are interested in modeling the dynamics of thin films and consider the effects of attractive van der Waals forces.

We introduce a rectangular coordinate system $\mathbf{x} = (x, y)$ with associated velocity field $\mathbf{u} = (u, v)$ for the liquid. The surrounding medium is taken to be passive as regards the fluid dynamics. The interface is allowed to deform and we define $H(x, t)$ to be half of the symmetrically perturbed layer thickness; d is the half mean thickness of the layer, as introduced earlier.

The governing equations consist of the Navier-Stokes equations and the continuity equation for the fluid layer, and Laplace equations for the voltage in each phase. In what follows we denote the liquid layer by region I and the surrounding medium by region II. In terms of our coordinates, these regions are defined laterally by $0 \leq y \leq H(x, t)$ and $y \geq H(x, t)$, respectively. In dimensional form these equations are

$$\rho(\mathbf{u}_t + \mathbf{u} \cdot \nabla \mathbf{u}) = -\nabla(P + \Phi) + \mu \nabla^2 \mathbf{u}, \tag{1}$$

$$\nabla \cdot \mathbf{u} = 0, \tag{2}$$

$$\nabla^2 V^{I,II} = 0. \tag{3}$$

The disjoining potential Φ has been included to model van der Waals attractive forces and this is taken to be proportional to $1/H^3$ (see for example Erneux and Davis[13]) and is defined more precisely later. The electric fields are $\mathbf{E}^{I,II} = -\nabla V^{I,II}$.

Equations (1)-(3) must be solved subject the symmetry conditions

$$u_y(x, 0, t) = v(x, 0, t) = 0, \quad V_y^I(x, 0, t) = 0, \tag{4}$$

at the centerline, and the potential far from the sheet must tend to its undisturbed value,

$$V^{II} \to \frac{V_0}{2L} x \quad \text{as} \quad y \to \infty. \tag{5}$$

In addition, we must satisfy interfacial boundary conditions at $y = H(x, t)$. These are a kinematic condition

$$v = H_t + u H_x, \tag{6}$$

tangential and normal stress balances

$$[\mathbf{t} \cdot \mathbf{T} \cdot \mathbf{n}]_{II}^{I} = 0, \tag{7}$$

$$[\mathbf{n}\cdot\mathbf{T}\cdot\mathbf{n}]_{II}^{I}=\frac{\sigma H_{xx}}{(1+H_x^2)^{\frac{3}{2}}},\tag{8}$$

continuity of normal components of the electric displacement

$$\mathbf{n}\cdot[\epsilon\mathbf{E}]_{II}^{I}=0.\tag{9}$$

and continuity of tangential components of the electric field

$$\mathbf{n}\times[\mathbf{E}]_{II}^{I}=0.\tag{10}$$

In the above boundary conditions we have introduced the jump notation $[*]_{II}^{I}=(*)^{I}-(*)^{II}$. Here, σ is the constant surface tension coefficient, $\mathbf{n}$ and $\mathbf{t}$ are the outward pointing normal and tangent to the interface, respectively, and the stress tensor $\mathbf{T}$ is given by

$$T_{ij}=-P\delta_{ij}+\mu\left(\frac{\partial u_i}{\partial x_j}+\frac{\partial u_j}{\partial x_i}\right)+\epsilon\left(E_iE_j-\frac{1}{2}|\mathbf{E}|^2\delta_{ij}\right).\tag{11}$$

The last term in (11) comes from the Maxwell stresses at the interface[24]. It can be shown, and this is used later, that the Maxwell stresses do not contribute to the tangential stresses but affect normal stresses alone. This is done by considering $[\mathbf{t}\cdot\mathbf{T}_E\cdot\mathbf{n}]_{II}^{I}$, where $\mathbf{T}_E$ is the electric part of the tensor (11), and using the electric field boundary conditions (9) and (10) to show that the jump is identically equal to zero.

The equations are made dimensionless by scaling horizontal distances with L and vertical ones with d. Introducing a typical velocity scale U (this could be a capillary or viscous based velocity, for example - see[13] for the latter), and the slenderness parameter $\varepsilon=d/L$, the following scales are adopted (primes denote dimensionless variables and will subsequently be dropped):

$$\begin{aligned}x=Lx',\quad y=dy',\quad (u,v)=U(u',\varepsilon v'),\quad t=\frac{L}{U}t'\\ P=\rho U^2P'\ ,\ \Phi=\rho U^2\Phi'\ ,\text{ and } V=V_0V'.\end{aligned}\tag{12}$$

The dimensionless van der Waals potential can be expressed in terms of the local film thickness as $\Phi'=K(H_+-H_-)^{-3}$, where $K=K'/(6\pi\rho d^3U^2)$ is the non-dimensional van der Waals constant and K' is the Hamaker constant. Using the symmetry of the film, we write $H_+=-H_-\equiv H(x,t)$, to obtain

$$\Phi'=\frac{K}{8H^3}.\tag{13}$$

Substituting these scales into the governing equations and dropping primed quantities, provides dimensionless equations and boundary conditions. We develop these in terms of a

dimensionless perturbation voltage (note that this can be as large as the base voltage - no linearizing approximation is made) defined by

$$V^{I,II} = \frac{x}{2} + \tilde{V}^{I,II}. \tag{14}$$

The Navier-Stokes, continuity and Laplace equations for the voltage are

$$u_t + uu_x + vu_y = -(P+\Phi)_x + \frac{1}{Re}(u_{xx} + \frac{1}{\varepsilon^2}u_{yy}), \tag{15}$$

$$\varepsilon^2\left(v_t + uv_x + vv_y\right) = -(P+\Phi)_y + \frac{\varepsilon^2}{Re}(v_{xx} + \frac{1}{\varepsilon^2}v_{yy}), \tag{16}$$

$$u_x + v_y = 0 \tag{17}$$

$$\varepsilon^2\tilde{V}^{I,II}_{xx} + \tilde{V}^{I,II}_{yy} = 0. \tag{18}$$

The symmetry boundary conditions are

$$u_y(x,0,t) = v(x,0,t) = 0, \quad \tilde{V}^I_y(x,0,t) = 0, \tag{19}$$

and at $y = H(x,t)$ we have the kinematic condition, tangential stress balance, normal stress balance, continuity of normal components of the electric displacement, and continuity of tangential components of the electric field, which are:

$$v = H_t + uH_x, \tag{20}$$

$$2\varepsilon^2 H_x\left(v_y - u_x\right) + \left(1-\varepsilon^2 H_x^2\right)\left(u_y + \varepsilon^2 v_x\right) = 0. \tag{21}$$

$$\begin{aligned} -P \;+\; & \frac{2}{Re(1+\varepsilon^2H_x^2)}\left\{u_x(\varepsilon^2H_x^2-1) - H_x(u_y+\varepsilon^2v_x)\right\} \\ & + \frac{1}{1+\varepsilon^2H_x^2}E_b\left\{\varepsilon^2H_x^2\left[\frac{\epsilon}{2}\left(\frac{1}{4}+\tilde{V}_x+\tilde{V}_x^2\right) - \frac{\epsilon}{2}\frac{\tilde{V}_y^2}{\varepsilon^2}\right]_{II}^{I}\right. \\ & \left. - 2H_x\left[\epsilon\left(\frac{1}{2}+\tilde{V}_x\right)\tilde{V}_y\right]_{II}^{I} + \left[\frac{\epsilon}{2}\frac{\tilde{V}_y^2}{\varepsilon^2} - \frac{\epsilon}{2}\left(\frac{1}{4}+\tilde{V}_x+\tilde{V}_x^2\right)\right]_{II}^{I}\right\} \\ & \frac{\varepsilon}{CaRe}\frac{H_{xx}}{(1+\varepsilon^2H_x^2)^{\frac{3}{2}}} \end{aligned} \tag{22}$$

$$\epsilon_p\left[\varepsilon^2H_x\left(\frac{1}{2}+\tilde{V}_x^I\right) - \tilde{V}_y^I\right] = \varepsilon^2H_x\left(\frac{1}{2}+\tilde{V}_x^{II}\right) - \tilde{V}_y^{II}, \tag{23}$$

$$H_x\tilde{V}_y^I + \tilde{V}_x^I = H_x\tilde{V}^{II} + \tilde{V}_x^{II}. \tag{24}$$

The perturbation potential must vanish at infinity, giving

$$\tilde{V}^{II} \to 0 \quad \text{as} \quad y \to \infty. \tag{25}$$

The dimensionless groups appearing in the equations are a Reynolds number Re, a capillary number Ca, the relative permittivity ϵ_p and an electric capillary number E_b. These are given by

$$Re = \frac{\rho U L}{\mu}, \quad Ca = \frac{\mu U}{\sigma}, \quad \epsilon_p = \frac{\epsilon^I}{\epsilon_o}, \quad E_b = \frac{V_0^2}{L^2}\frac{1}{\rho U^2}. \tag{26}$$

The dimensionless problem given above, along with initial conditions, constitutes a nonlinear free-boundary problem whose evolution can terminate in finite-time singularities if the sheet ruptures. The above scalings are exact transformations, and the case $\varepsilon = 1$ recovers the system when the vertical and horizontal scales are of the same order. The linear stability of the full system treating, ε as an order one parameter, is described in the Appendix. The limit $\varepsilon \to 0$ corresponds to long waves whose nonlinear evolution we analyze next, by deriving and solving a system of evolution equations. The linear stability of the evolution equations recovers the $\varepsilon \ll 1$ limit of the linear stability of the full system, as expected.

III. NONLINEAR EVOLUTION EQUATIONS

In what follows we give a brief description of the derivation of the evolution equations that we use to study the nonlinear stability of this flow. For details regarding matching between inner and outer solutions of the electric field, we refer the reader to our study of the inviscid problem in Tilley et al.[23]. As shown in the Appendix, the relevant limits are given by (A.7), and we write

$$Ca = \frac{\varepsilon}{\Sigma}, \quad E_b = \frac{\bar{E}_b}{\varepsilon}, \tag{27}$$

where Σ and $\bar{E}_b$ are order one quantities. The asymptotic solution for the voltage potential follows the same lines as in[23]. It is found that solutions must be constructed in the following three regions: (i) inside the fluid layer, $0 < y < H(x,t)$ (region I), (ii) outside the fluid layer but at order one distance, $H(x,t) < y \ll \infty$ (region II), and, (iii) far away from the fluid layer $y \sim \frac{1}{\varepsilon}$ (region III). Region III needs to be incorporated into the solution procedure in order to allow the boundary condition on the voltage at infinity to be satisfied. This is achieved by bringing in the horizontal derivative terms of the Laplacian, which are small in regions I and II where $y = O(1)$. Solutions are obtained in each of the three regions and matching between regions II and III provides the leading order solutions required to find

the Maxwell stress contribution to the normal stress balance. Details of this matching can be found in[23]. The asymptotic solutions needed in our analysis are, then,

$$V^I = \frac{x}{2} + \varepsilon \tilde{V}_1^I + O(\varepsilon^2), \qquad V^{II} = \frac{x}{2} + \varepsilon \tilde{V}_1^{II} + O(\varepsilon^2),$$

$$\tilde{V}_1^I = \tilde{V}_1^{II} = \frac{1-\epsilon_p}{2}\mathcal{H}(H_0), \tag{28}$$

where $\mathcal{H}$ is the Hilbert transform operator given by

$$\mathcal{H}(f(x)) = \frac{1}{\pi} PV \int_{-\infty}^{\infty} \frac{f(y)}{x-y} dy,$$

where PV denotes the principal value of the integral. We note that the Hilbert transform term arises naturally in the solution of the outer problem (region III), in terms of the Green's function of Laplace's equation in two dimensions. Our analysis uses Fourier transforms to solve the relevant Dirichlet problem and the matching is done in Fourier space. Inversion to real space results in equation (28).

The appropriate asymptotic expansions for the fluid dynamics are

$$u = u_0 + \varepsilon u_1 + \varepsilon^2 u_2 + \ldots, \tag{29}$$
$$v = v_0 + \varepsilon v_1 + \varepsilon^2 v_2 + \ldots, \tag{30}$$
$$P = P_0 + \varepsilon P_1 + \ldots, \tag{31}$$
$$H = H_0 + \varepsilon H_1 + \ldots, \tag{32}$$
$$\Phi = \Phi_0 + \varepsilon \Phi_1 + \ldots. \tag{33}$$

Substitution of these into the governing equations (15)-(17) along with use of the symmetry conditions at $y = 0$ gives the following leading order velocities

$$u_0 = C(x,t), \qquad v_0 = -yC_x, \tag{34}$$
$$u_1 = C_1(x,t), \qquad v_1 = -yC_{1x},$$

with the leading order horizontal velocity $C(x,t)$ to be determined. We note that without loss of generality, the velocities u_1 and v_1 (i.e. $C_1(x,t)$) can be set to zero by redefinition of the functions $C(x,t)$. The normal stress balance condition (22) (with the distinct scalings (27) introduced above) gives, to leading order,

$$-P_0 - \frac{2}{Re} H_{0x} u_{0y} + \frac{2}{Re} v_{0y} + \bar{E}_b \left\{ 2H_{0x} \left[\frac{\epsilon}{2} \tilde{V}_{1y} \right]_{II}^{I} + \left[\epsilon \tilde{V}_{1y} \tilde{V}_{2y} \right]_{II}^{I} - \left[\frac{\epsilon}{2} \tilde{V}_{1x} \right]_{II}^{I} \right\} = \frac{\Sigma}{Re} H_{0xx}, \tag{35}$$

which on introduction of the appropriate solutions from (34) and (28) gives an equation for the leading order pressure P_0,

$$-P_0 - \frac{2}{Re}C_x + \frac{1}{4}\epsilon_0(1-\epsilon_p)^2\mathcal{H}(H_{0x}) = \frac{\Sigma}{Re}H_{0xx}. \tag{36}$$

On use of the leading order solutions (34) into the leading order y-momentum equation, implies that $(P_0+\Phi_0)_y = 0$, and hence $P_0+\Phi_0 = D(x,t)$; the function $D(x,t)$ can be found by evaluating the pressure at the interface $y = H_0$ as given by equation (35). This yields

$$D(x,t) = -\frac{2}{Re}C_x + \frac{1}{4}\epsilon_0(1-\epsilon_p)^2\mathcal{H}(H_{0x}) - \frac{\Sigma}{Re}H_{0xx} - \Phi_0, \tag{37}$$

where $\Phi_0 = K/(8H_0^3)$. The x-momentum equation (15) at the next order gives

$$u_{2yy} = Re\,(C_t + CC_x + D_x) - C_{xx},$$

which when integrated once and use is made of the symmetry condition $u_{2y}(x,0,t) = 0$, gives

$$u_{2y} = yRe\,\{C_t + CC_x + D_x\} - yC_{xx}. \tag{38}$$

The system is closed by considering the leading order contribution (which is $O(\varepsilon^2)$) of the tangential stress balance equation (21) which is

$$u_{2y} + v_{0x} - u_{0y}H_{0x}^2 - 4u_{0x}H_{0x} = 0 \qquad \text{at} \quad y = H_0(x,t). \tag{39}$$

Substitution of u_{2y} from (38) into (39) and elimination of $D(x,t)$ by use of (37), provides an evolution equation connecting $C(x,t)$ and $H_0(x,t)$. Another equation follows from the leading order contribution to the kinematic condition (20), and physically corresponds to conservation of mass. The system is (written in reverse order)

$$H_{0t} + (CH_0)_x \;=\; 0, \tag{40}$$

$$C_t + CC_x \;=\; \frac{4}{Re}\frac{(H_0C_x)_x}{H_0} - \Phi_{0x} - \frac{\epsilon_0}{4}\bar{E}_b(1-\epsilon_p)^2\mathcal{H}(H_{0xx}) + \frac{\Sigma}{Re}H_{0xxx}. \tag{41}$$

where

$$\Phi_0 = \frac{K}{8(H_0(x,t))^3}. \tag{42}$$

In addition, boundary and initial conditions must also be specified. In the numerical work that follows we adopt periodic boundary conditions which are well-suited for accurate pseudo-spectral calculations.

Before proceeding to such calculations, we consider the linear stability of the evolution equations and compare with the results in the Appendix. Linearizing about $H_0 = 1$ and $C = 0$, and looking for normal modes proportional to $e^{ikx+\omega t}$, we find the dispersion relation

$$\omega^2 + 4\frac{k^2}{Re}\omega - \frac{3}{8}k^2K + \bar{E}_b\frac{\epsilon_o}{4}(1-\epsilon_p)^2k^2|k| + \frac{\Sigma}{Re}k^4 = 0. \tag{43}$$

This is identical with the limiting dispersion relation (A.6) found by starting from the full problem, making a long wave approximation as ε becomes small, and using the limiting forms (27) identified in the Appendix. Writing

$$W_f = \frac{\Sigma}{Re}, \qquad W_e = \bar{E}_b\frac{\epsilon_0}{4}(1-\epsilon_p)^2, \tag{44}$$

the solutions of (43) are

$$\omega = \frac{-\frac{4k^2}{Re} \pm \sqrt{\frac{16k^4}{Re^2} - 4\left[-\frac{3}{8}k^2K + W_fk^4 + W_ek^2|k|\right]}}{2}. \tag{45}$$

The solution with the positive sign for the square root can give rise to instability, while the other root is always stabilizing. The expression for ω shows that surface tension (which appears through the parameter W_f), and the electic field (appearing through the parameter W_e), stabilize the flow, as opposed to van der Waals forces which are destabilizing. As W_e increases, the band of unstable modes as well as the maximum growth rate decrease. The critical wavenumber, k_c say, above which the flow is stable, can be found by inspection of the term under the square root in equation (45), which indicates that if the term in the square bracket is greater than zero, then the real part of ω is negative for all k and so a complete stabilization follows. The value of k_c is found by setting $-\frac{3}{8}k^2K + k^4W_f + k^3W_e = 0$, which gives

$$k_c = \frac{-W_e + \sqrt{W_e^2 + \frac{3}{2}W_fK}}{2W_f}. \tag{46}$$

The expression (46) shows immediately that in the absence of an electric field, the band of unstable modes has size $(3K/8W_f)^{\frac{1}{2}}$ and so the flow becomes unstable to shorter wavelengths as K is increased and/or W_f is decreased, as would be expected on physical grounds. What is more interesting, however, is the stabilization provided by the electric field. As W_e increases the critical wavenumber decreases and the behavior for large W_e is $k_c \sim \frac{3K}{8W_e}$.

In our numerical experiments we consider 2π-periodic boundary conditions. The wavenumbers are then integers and a Fourier series representation is appropriate in a straghtforward manner. If $k_c < 1$, the flow with these boundary conditions, is linearly stable. This leads to the following condition of linear stabilization

$$W_e > \frac{3}{8}K - W_f, \tag{47}$$

which provides a threshold value for the electric field parameter. As we show numerically in the following Section, the initial value problem with small data and values of W_e just below or above the threshold value (47), terminates in either rupture or a relaxation (after a long time) to the flat uniform state.

In the numerical work that follows we re-write the dependent variables in the evolution equations (40) and (41) according to

$$H_0 \to H, \quad C \to u,$$

and use the definitions (44).

IV. NUMERICAL SOLUTION OF THE EVOLUTION EQUATIONS

We now address the long-wave nonlinear evolution problem (40)-(41) numerically. The equations are solved on 2π-periodic domains and the initial conditions are taken to be of the form

$$H(x,0) = 1 + h_0 \cos(x), \qquad u(x,0) = u_0 \sin(x). \tag{48}$$

The parameters h_0 and u_0 are initial amplitudes and the geometry of the problem necessitates $0 < h_0 < 1$. The symmetry of the initial conditions is preserved by the evolution equations and this choice has been made in order to have some prior knowledge regarding the place of singularity formation (sheet rupture), for example. An additional accuracy check for the numerical work arises from integration of (40) over one period; in our double-precision simulations we find

$$\frac{d}{dt}\int_0^{2\pi} H(x,t)dx = O(10^{-15}). \tag{49}$$

Also, momentum is conserved by (40)-(41). To see this, multiply (41) by H_0 and integrate over one period. The quantity $H_0 C$ is conserved in time provided $\int H_0 \mathcal{H}(H_{0xx})dx = 0$; one way to show this is by considering

$$\int_{-\infty}^{\infty} H_0 \mathcal{H}(H_{0xx})dx = \mathcal{F}(H_0 \mathcal{H}(H_{0xx}))|_{k=0} = -i\left\{\int_{-\infty}^{\infty} \hat{H}_0(k-\xi)\xi^2 \mathrm{sgn}(\xi)\hat{\mathrm{H}}_0(\xi)\mathrm{d}\xi\right\}_{k=0}, \tag{50}$$

where $\mathcal{F}$ is the Fourier transform and k is the wavenumber variable. It follows that $\int H_0 \mathcal{H}(H_{0xx})dx = 0$ because the last integrand in (50) is odd with respect to ξ. In our double-precision numerical simulations we find

$$\int_0^{2\pi} H(x,t)u(x,t)dx = O(10^{-16}), \tag{51}$$

which is in agreement with the initial conditions (48).

The numerical solutions presented here are carried out using a pseudo-spectral method in space and a four-stage Runge-Kutta method in time. The time step is adaptive and depends on the number of spatial modes whose amplitudes are greater than some prescribed tolerance, typically between 10^{-9} and 10^{-11}. Further, the solution is spectrally interpolated when $N/2-5$ modes have an amplitude larger than this prescribed criterion, where N is the number of collocation points. The accuracy requirement can be quite severe due to dispersive terms in the dispersion relation, even though all sufficiently large wavenumbers are damped by the viscous terms. This is especially felt at large values of W_f and one way to see this is to drop the viscous term (i.e., formally set $R_e = \infty$). Then, the dispersion relation for large wavenumbers k provides solutions proportional to $\exp(ikx \pm ik^2 {W_f}^{1/2} t)$ irrespective of the value of $W_e = O(1)$; these solutions rotate the Fourier modes in the complex plane and to control such rotations we require $k^2 \Delta t < \nu$, where ν is sufficiently small and is between 0.1 and 0.8 in our calculations. The code maintains this accuracy restriction throughout the course of a numerical simulation which terminates upon satisfaction of a comparison of $H(\pi, t)$ with 5×10^{-3}.

A. Code Validation

As an accuracy test and an evaluation of the code, we consider the case of zero electric field, $W_e = 0$. This problem has been solved numerically in[18], and we reproduce those results first by setting $W_e = 0$. In the calculations of[18], the periodic domain is taken to be $[-1, 1]$ and their equivalent of our equation (41) is

$$u_t + uu_x = \frac{4}{H}(Hu_x)_x - (H^{-3})_x + 3Sh_{xxx}, \tag{52}$$

where S is their surface tension parameter. Our 2π-periodic domains, and different non-dimensionalization, make it necessary to take the following parameter values in order to make a direct comparison

$$R_e = \frac{1}{\pi}, \quad K = 8, \quad W_f = \frac{3}{2}. \tag{53}$$

In addition, the appropriate initial conditions for these comparisons are $h_0 = 0.2$ and $u_0 = -0.1$. The original numerical study of the zero electric field problem[14] suggested the formation of similarity solutions of the second type near rupture. The computations of[18], however, were able to resolve the fast dynamics near pinching using adaptive gridding techniques, and give strong support to similarity solutions of the first kind with the dominant balances being between inertia, viscosity and van der Waals forces, with surface tension forces being negligible near rupture. It has been suggested, and was confirmed numerically[18], that

the following similarity solutions hold near the singular time t_s and rupture point $x = x_s$,

$$H(x,t) = \tau^{\alpha} F(\eta), \qquad u(x,t) = \tau^{\gamma} G(\eta), \qquad \eta = \frac{x - x_s}{\tau^{\beta}}, \tag{54}$$

where $\tau = t_s - t$ and the constants α, β, and γ are scaling exponents to be determined. We note that the similarity solutions of[14], which balance van der Waals forces with viscosity while inertia and surface tension are both subdominant, give $\alpha = 1/3$ with β left undetermined. Balancing all terms besides surface tension, however, determines all exponents, and these are given by

$$\alpha = \frac{1}{3}, \quad \beta = \frac{1}{2}, \quad \gamma = -\frac{1}{2}. \tag{55}$$

The scaling exponents (55) and the similarity solutions (54), can be confirmed numerically by plotting appropriate variables on log-log scales. Following[18], we graphed $max_{x\in(0,2\pi)}\{u_x(x,t)\}$, $-H_t(\pi,t)$ and $max_{x\in(0,2\pi)}\{u(x,t)\}$ against the minimum film thickness, $H(\pi,t)$. Our estimates of the similarity exponents appear in Table I where they are compared to the theoretically predicted values (55). Our other numerical output reproduces accurately the calculations in[18]. For example, the time to rupture according to our results is $t_s = 4.78437956$ and dividing this by π due to the difference in time scales between our simulations and those in[18], we obtain $t_* \sim 1.5229...$ in complete agreement with the value given in Section IIIA of[18].

B. Large-amplitude Inital Data

We consider next the inclusion of the electric field into the nonlinear evolution of large-amplitude ($h_0 = 0.2$, $u_0 = -0.1$) initial data. The remaining parameters are chosen as follows: $Re = 1$, $K = 8$, $W_f = 1$ and W_e is varied.

We note, first, that the similarity solutions and scales (54) and (55) are still consistent structures as a singularity forms. To see this, we can use these solutions to estimate the size of the electric field term compared to the terms retained, and find that it is asymptotically smaller; this must be so, since the electric field effects are asymptotically smaller than surface tension forces as rupture develops, and the latter are excluded from the main balances also. We begin, therefore, with a typical situation and aim to confirm numerically the similarity solutions described above. Figures 1-2 show profiles for $W_e = 0$ which are identical to those we obtained for $W_e > 0$ (not shown here for the sake of brevity). Figure 3 shows the data used to determine the exponents given in Table II thus verifying the assertion above, that the $W_e = 0$ ruptured solutions remain the attractor of the solution when $W_e > 0$.

A rather interesting result (obtained numerically) is shown in Figure 4. In the fully nonlinear regime there exists a critical value for W_e (the electric field) which removes the rupturing

solutions. At values lower than this critical W_e (whose value is directly proportional to the initial energy input through h_0 and u_0) the film evolves to a finite time singularity. Assuming a similarity law for the dependence of t_s on W_e, i.e., $t_s = O([W_e^* - W_e]^{-k})$, we estimated (see Figure 5) $W_e^* \approx 2.613408$ and $k \approx 0.1244$.

C. Small-amplitude Initial Data

The stabilization effect of the electric field, for which the threshold value $W_e = 2$ is determined with the linear stability analysis (see Section 3), is now investigated. We set $h_0 = 0.01$ and $u_0 = 0$ and consider two cases. The first just above threshold and having $W_e = 2.05$, and the second just below threshold with $W_e = 1.95$. We expect the former solution to be stable and to evolve to a uniform quiescent state, while the latter should rupture at finite time. This is indeed the case as Figure 6 shows. We also observe from Figure 6 a long adjustment of the flow until the weak linear instability has a chance to amplify the flow into the nonlinear regime and rupture. The rupture time is approximately equal to 152.98415. For $W_e = 1.95$ we report in Table III the similarity exponents extracted from the data displayed in Figure 7.

Finally, Figure 8 shows the manner in which the interface shape relaxes to the basic state $H(x,t) = 1$ when W_e is above the threshold indicated by the linear stability analysis.

V. CONCLUSIONS

In the present work we examined the effect of an axial electric field on the rupture dynamics of a thin viscous liquid film subject to attractive van der Waals molecular forces. The liquid was assumed to be non-conducting electrically. This was undertaken in order to determine whether the electric field can be used as an additional control parameter in applications where rupture of the thin liquid film is an undesirable outcome.

Our study begun with the two-dimensional Navier-Stokes equations for the fluid motion coupled to Laplace equations for the electric field potentials. The two physical problems are coupled through polarization forces that develop at the interface between the liquid and the surrounding passive medium. A linear stability analysis of the resulting set of equations was performed. We determined that one can always choose a value of the electric field magnitude (through the electric capillary number) so that a linearly unstable flow (due to the attractive van der Waals force) is stabilized. Also, a long-wave asymptotic analysis of the full set of equations was performed in order to determine the nonlinear stability properties of perturbations of the (flat) basic state of the flow. A pseudo-spectral solver was employed to numerically simulate rupturing films and determine the effect of the electric field on the

dynamics of the process. Significantly, we found that the rupturing solution in the presence of an electric field exhibits similarity of the first-kind which is delayed relative to the case of rupture in the absence of electric forces. Further, we determined and verified the presence of an electric field amplitude past which the van der Waals unstable flow is completely regularized in the long-wave regime.

Acknowledgements

DTP was supported by the National Science Foundation, Grants DMS-9904793 and DMS-0072228. PGP was supported by a Grant from the Air Force Office of Scientific Research, AFOSR Grant no. F49620-02-1-0031. BST was supported by the National Science Foundation, DMS-9971383.

APPENDIX

The linear stability of equations (15)-(18) and boundary conditions (20)-(24) is carried out by looking for normal mode solutions in the form

$$\left(\psi, H, \tilde{V}^{I,II}, P\right) = \left(\delta\hat{\psi}(y), 1+\delta H_0, \delta\hat{V}^{I,II}(y), P_0+\delta\hat{P}(y)\right)\exp(ikx+\omega t), \tag{A.1}$$

where $0 < \delta \ll 1$ is a linearization amplitude and $\psi(x,y,t)$ is the Stokes stream function so that $u = \psi_y$, $v = -\psi_x$. Such a temporal stability analysis has been carried out, in the absence of surface tension, by Melcher and Schwarz[19]. A dispersion relation follows after some algebra which involves solving for the perturbation stream function inside the film and the voltage potentials inside and outside the film, and applying the linearized boundary conditions to eliminate constants of integration. The eigenfunctions can be written in terms of two constants A and B as follows:

$$\hat{\psi}(y) = A\left(\sinh(\varepsilon y\sqrt{k^2+\omega Re}) - \frac{(2k^2+\omega Re)\sinh(\varepsilon\sqrt{k^2+\omega Re})}{2k^2\sinh(\varepsilon k)}\sinh(\varepsilon k y)\right), \tag{A.2}$$

$$\hat{V}^I(y) = B\cosh(\varepsilon k y), \quad \hat{V}^{II}(y) = C\cosh(\varepsilon k)e^{-\epsilon k(y-1)}, \tag{A.3}$$

$$H_0 = \frac{iARe\sinh(\varepsilon\sqrt{k^2+\omega Re})}{2k}. \tag{A.4}$$

The linearized normal stress boundary condition and the continuity of the normal component of the electric displacement, provide two linear homogeneous equations for A and B and non-trivial solutions are possible as long as the following dispersion relation is satisfied:

$$\omega^2 + 4\frac{\omega k^2}{Re} - 4\frac{k^3}{Re^2}\sqrt{k^2+\omega Re}\coth(\varepsilon\sqrt{k^2+\omega Re})\tanh(\varepsilon k) +$$
$$4\frac{k^4}{Re^2} + \frac{1}{CaRe}k^3\tanh(\varepsilon k) - \frac{3}{8}\frac{kK}{\varepsilon}\tanh(\varepsilon k) + \frac{E_b\epsilon_o k^2\sinh(\varepsilon k)(\epsilon_p-1)^2}{4(\epsilon_p\sinh(\varepsilon k)+\cosh(\varepsilon k))} = 0. \qquad \text{(A.5)}$$

This equation must be solved to obtain $\omega(k)$ and instability results if $Real(\omega) > 0$. The equation is implicit for ω and in fact an infinite number of solutions are possible for each k - this follows from the transcendental nature of the equation. The objective is to determine the value(s) of k which provide the most unstable waves with the maximum growth rate. Solutions can be obtained numerically using root-finding methods. It is found that as the electric field parameter E_b increases (with the other parameters held fixed), the maximum growth-rate decreases and its corresponding wavelength shifts to larger values. In addition, the cut-off wavenumber above which the flow is linearly stable, decreases algebraically with increasing E_b. This suggests the possibility of using the electric field as a stabilizing control, and our interest lies in nonlinear stabilization of van der Waals forces.

The asymptotic expansions required in the development of a longwave nonlinear theory, can be deduced in a consistent manner from the analysis of the full dispersion relation (A.5). The relation is derived for a general aspect ratio ε, and the limit $\varepsilon \to 0$ follows readily and yields, to leading order,

$$\omega^2 + \frac{4}{Re}k^2\omega - \frac{3}{8}Kk^2 + \frac{\epsilon_0(\epsilon_p-1)^2\varepsilon E_b}{4}k^2|k| + \frac{\varepsilon}{CaRe}k^4 = 0. \qquad \text{(A.6)}$$

If we take Re to be an order one quantity (in fact Re can be scaled out of the problem and so without loss of generality can be taken to have unit value), then we observe from (A.6) that surface tension and electric field effects will be retained in this limit as long as

$$Ca \sim \varepsilon, \quad E_b \sim 1/\varepsilon. \qquad \text{(A.7)}$$

These scalings motivate the derivation of the nonlinear evolution equations of Section 3.

The long wave nonlinear problem in the absence of an electric field has been studied by Erneux and Davis[13]. For completeness we consider the generation of their dispersion relation by starting with our equation (A.6). The key to achieving this is to note the differences in non-dimensionalization. Erneux and Davis (ED from now) use $2d$ as the scale for lengths, $\nu/2d$ as the velocity scale, $4d^2/\nu$ to scale time and $\rho\nu^2/4d^2$ for the pressure scale. This implies that our Reynolds number $Re = 1/\varepsilon$ which casts (A.6), with $E_b = 0$, into

$$\omega^2 + 4\varepsilon k^2\omega - \frac{3}{8}Kk^2 + \frac{\varepsilon^2}{Ca}k^4 = 0. \qquad \text{(A.8)}$$

The changes in scales due to the different non-dimensionalizations can be used to obtain the ED dispersion relation from (A.8). More specifically, if we transform according to

$$\omega \to \frac{\omega}{\varepsilon}, \quad k \to \frac{k}{\varepsilon}, \quad Ca \to \frac{2}{3S},$$

the relation (A.8) recovers that of ED[13].

---

[1] M. Prevost and D. Gallez, *Nonlinear stability of thin free liquid films: rupture and Marangoni effects*, AIChE. Symp. Sur., **252**, (1986), pp. 123.

[2] M. Prevost and D. Gallez, *Nonlinear rupture of thin free liquid films*, J. Chem. Phys., **84**, (1986), pp. 4043.

[3] B.V. Deryagin, *The definition and magnitude of disjoining pressure and its role in statics and dynamics of thin films*, Colloid Journal USSR, **17**, (1955), pp. 207.

[4] J. Th. G. Overbeek, *Black soap films*, The Journal of Physical Chemistry, **64**, (1960), pp. 1178.

[5] A. Vrij, *Possible mechanism for the spontaneous rupture for thin free liquid films*, Discuss. Faraday Soc., **42**, (1996), pp. 23.

[6] E. Ruckenstein and R.K. Jain, *Spontaneus rupture of thin liquid films*, J. Chem .Soc. Faraday Trans. II, **70**, (1974), pp. 132.

[7] R.J. Gumerman, and G.M. Homsey, *The stability of radially bounded thin films*, Chem. Eng. Commun., **2**, (1975), pp. 27.

[8] M.B. Williams and S.H. Davis, *Nonlinear theory of thin film rupture*, J. Colloid Interface Sci., **90**, (1982), pp. 220.

[9] J.P. Burelbach, G. Bankoff and S.H. Davis, *Nonlinear stability of evaporating/condensing liquid films*, J. Fluid Mech., **195**, (1988), pp. 463.

[10] W.W. Zhang and J.R. Lister, *Similarity solutions for van der Waals rupture of a thin film*, Physics of fluids, **11**, (1999), pp. 2454.

[11] T.P. Witelski and A.J. Bernoff, *Stability of self-similarity solutions for van der Waals driven thin film rupture*, Physics of fluids, **11**, (1999), pp. 2443.

[12] A. Sharma and E. Ruckenstein, *Rupture of thin free films with insoluble surfactants: nonlinear aspects*, AIChE. Symp. Sur., **252**, (1986), pp. 130.

[13] T. Erneux and S.H. Davis, *Nonlinear rupture of free films*, Phys. Fluids A, **5**, No. 5, (1993), pp. 1117-1122.

[14] M.P. Ida and M.J. Miksis, *The dynamics of thin films I: General theory*, SIAM J. Appl. Math., **58**, No. 2, (1998), pp. 456-473.

[15] M.P. Ida and M.J. Miksis, *The dynamics of thin films II: Applications*, SIAM J. Appl. Math., **58**, No. 2, (1998), pp. 474-500.

[16] M.P. Ida and M.J. Miksis, *Thin film rupture*, Applied Math Letters, **9**, No.3, (1996), pp. 35-40.

[17] A. Oron, S.H. Davis and S.G. Bankoff, *Long-scale evolution of thin liquid films*, Reviews of Modern Physics, **69**, (1997), pp. 931-980.

[18] D. Vaynblat, J.R. Lister and T.P. Witelski, *Rupture of thin films by van der Waals forces: Evolution and self-similarity*, Phys. Fluids, **13**, (2001), pp 1130.

[19] J.R. Melcher and W.J. Schwarz, Jr., *Interfacial relaxation overstability in a tangential electric field*, Phys. Fluids, **11**, No. 12, (1968), pp. 2604-2616.

[20] M.F. El-Sayed, *Electro-aerodynamic instability of a thin dielectric liquid sheet sprayed with an air stream*, Phys. Rev. E, **60**, No. 6, (1999), pp. 7588-7591.

[21] H. Wendel, D. Gallez and P.M. Bisch, *On the dynamic stability of fluid dielectric films*, Journal of Colloid and Interface Science, **84**, No. 1, (1981), pp. 1.

[22] A. Gonzalez and A. Castellanos, *Nonlinear electrohydrodynamic waves on films falling down an inclined plane*, Phys. Rev. E, **53**, No. 4, (1996), pp. 3573-3578.

[23] B.S. Tilley, P.G. Petropoulos and D.T. Papageorgiou, *Dynamics and rupture of planar electrified liquid sheets*, Phys. Fluids, **13**, (2001), pp 3547.

[24] J.D. Jackson, *Classical Electrodynamics*, (1963), John Wiley and Sons, NY.

TABLE I: Our estimation of the scaling exponents of[18].

Quantity	Theoretical	Computed
u_x	$\frac{\gamma-\beta}{\alpha} = -3$	-2.98
$-H_t$	$\frac{\alpha-1}{\alpha} = -2$	-1.97
$max(u)$	$\frac{\gamma}{\alpha} = -1.5$	-1.50

TABLE II: Estimation of scaling exponents for $W_e = 2.2$, $u_0 = -0.1$ and $h_0 = 0.2$.

Quantity	Theoretical	Computed
u_x	$\frac{\gamma-\beta}{\alpha} = -3$	-2.97
$-H_t$	$\frac{\alpha-1}{\alpha} = -2$	-1.95
$max(u)$	$\frac{\gamma}{\alpha} = -1.5$	-1.47

TABLE III: Estimation of scaling exponents for $W_e = 1.95$, $u_0 = 0$ and $h_0 = 0.01$.

Quantity	Theoretical	Computed
u_x	$\frac{\gamma-\beta}{\alpha} = -3$	-2.95
$-H_t$	$\frac{\alpha-1}{\alpha} = -2$	-1.93
$max(u)$	$\frac{\gamma}{\alpha} = -1.5$	-1.50

LIST OF FIGURES

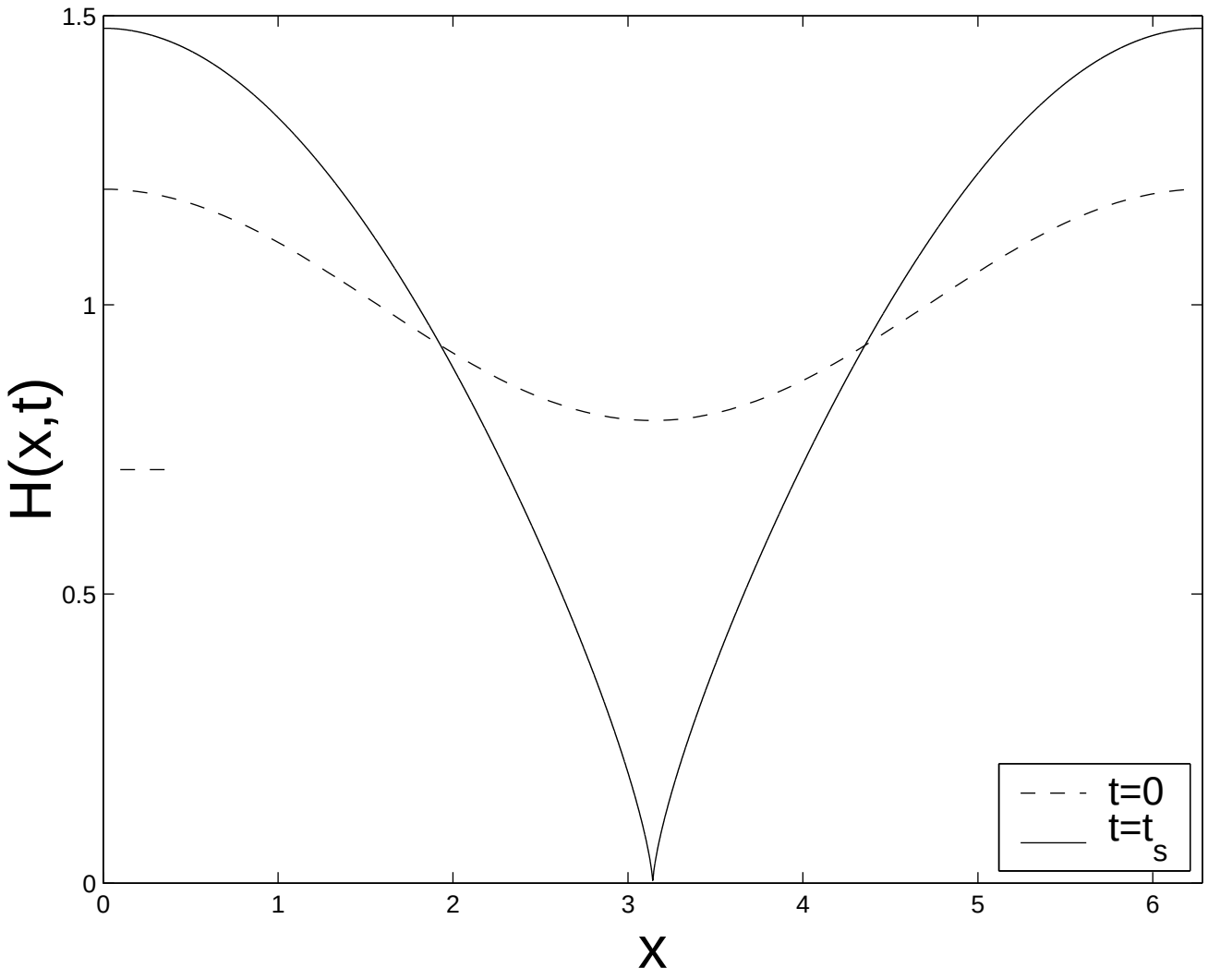

FIG. 1: Savettaseranee, Phys. Fluids

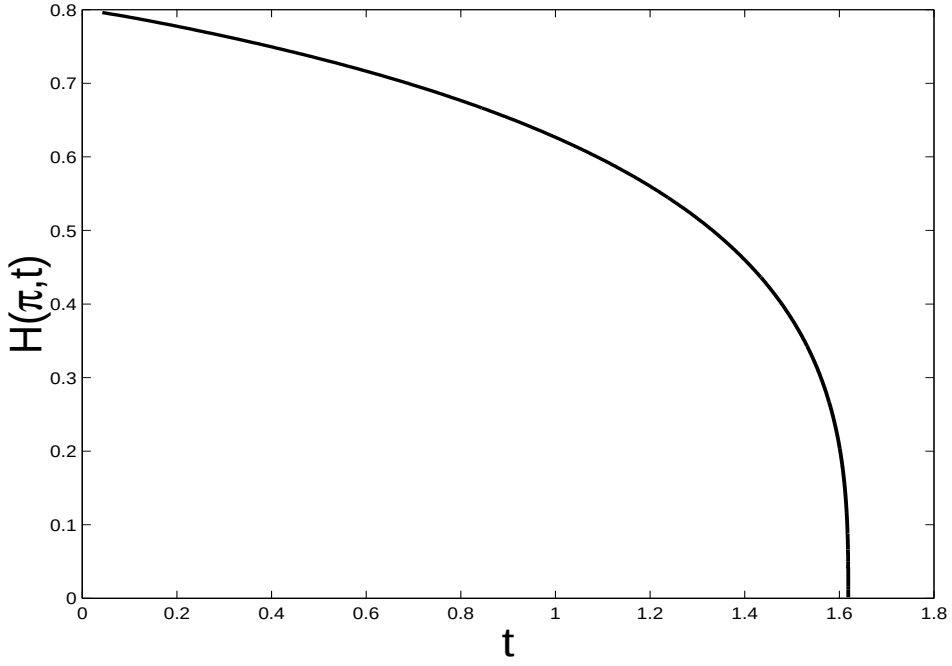

(a)

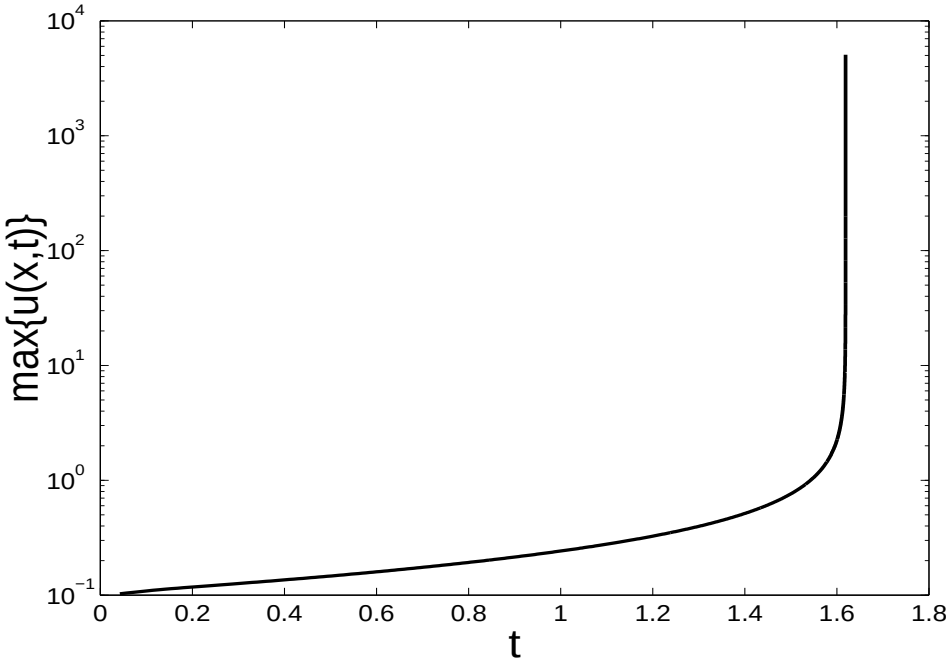

(b)

FIG. 2: Savettaseranee, Phys. Fluids

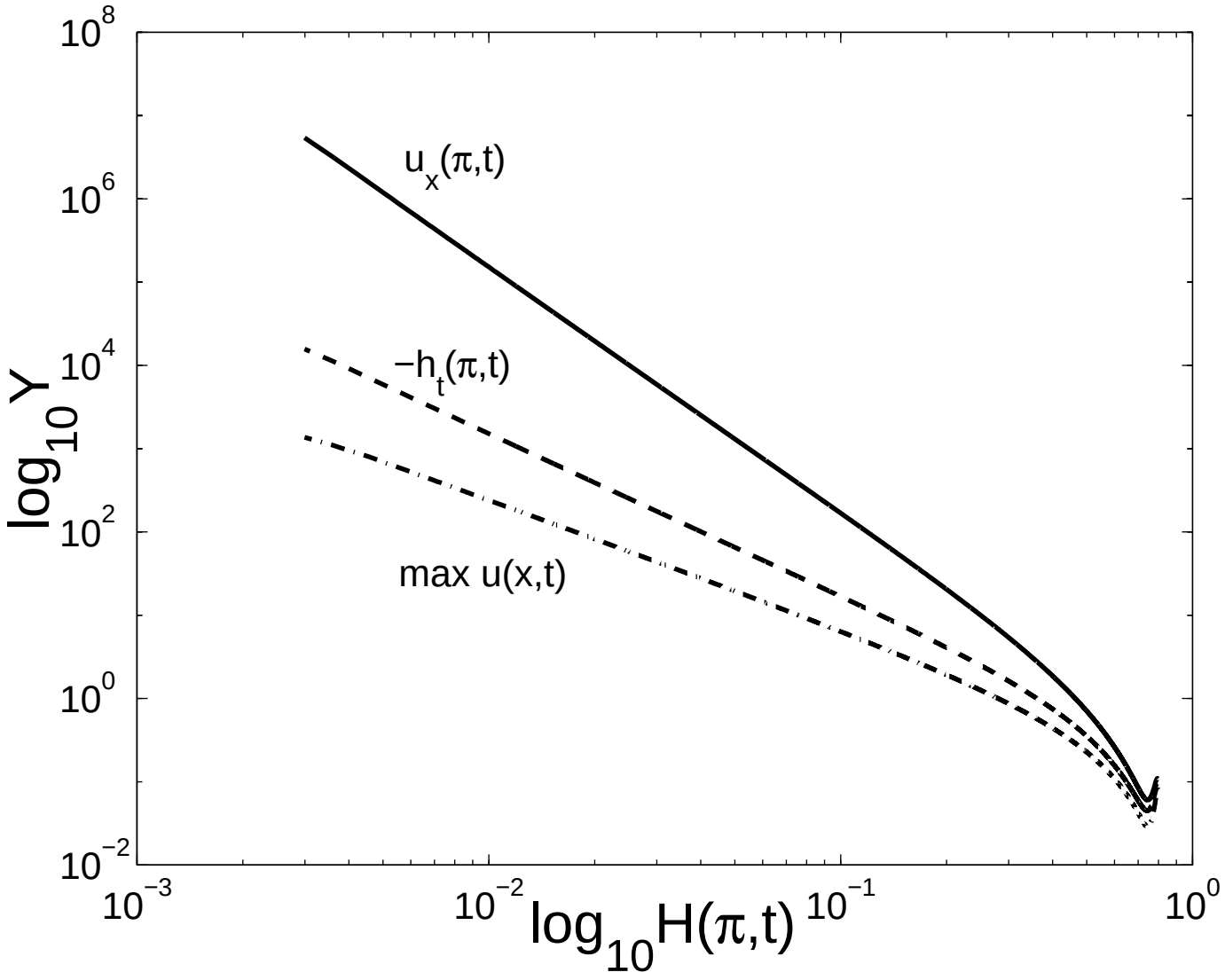

FIG. 3: Savettaseranee, Phys. Fluids

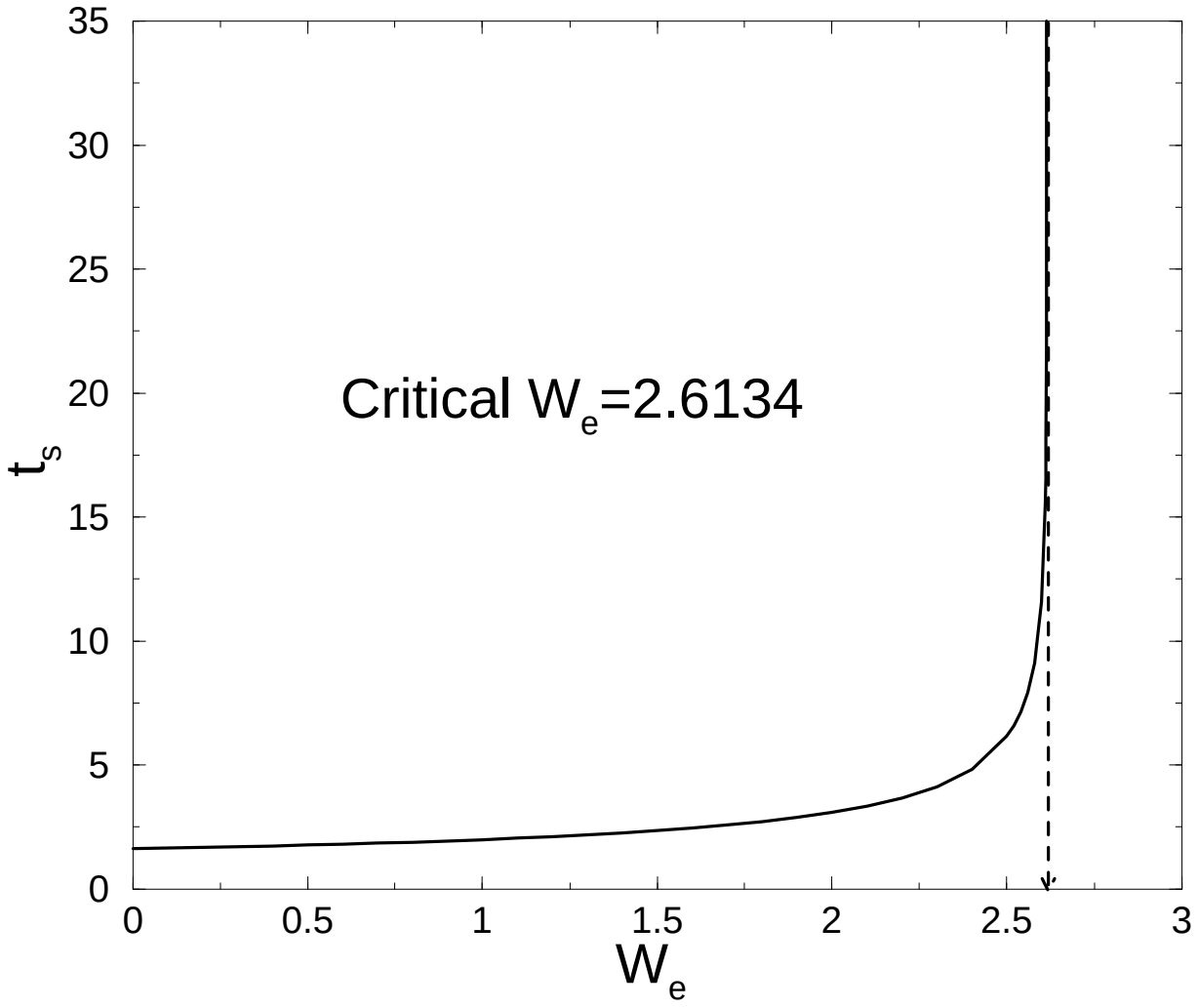

FIG. 4: Savettaseranee, Phys. Fluids

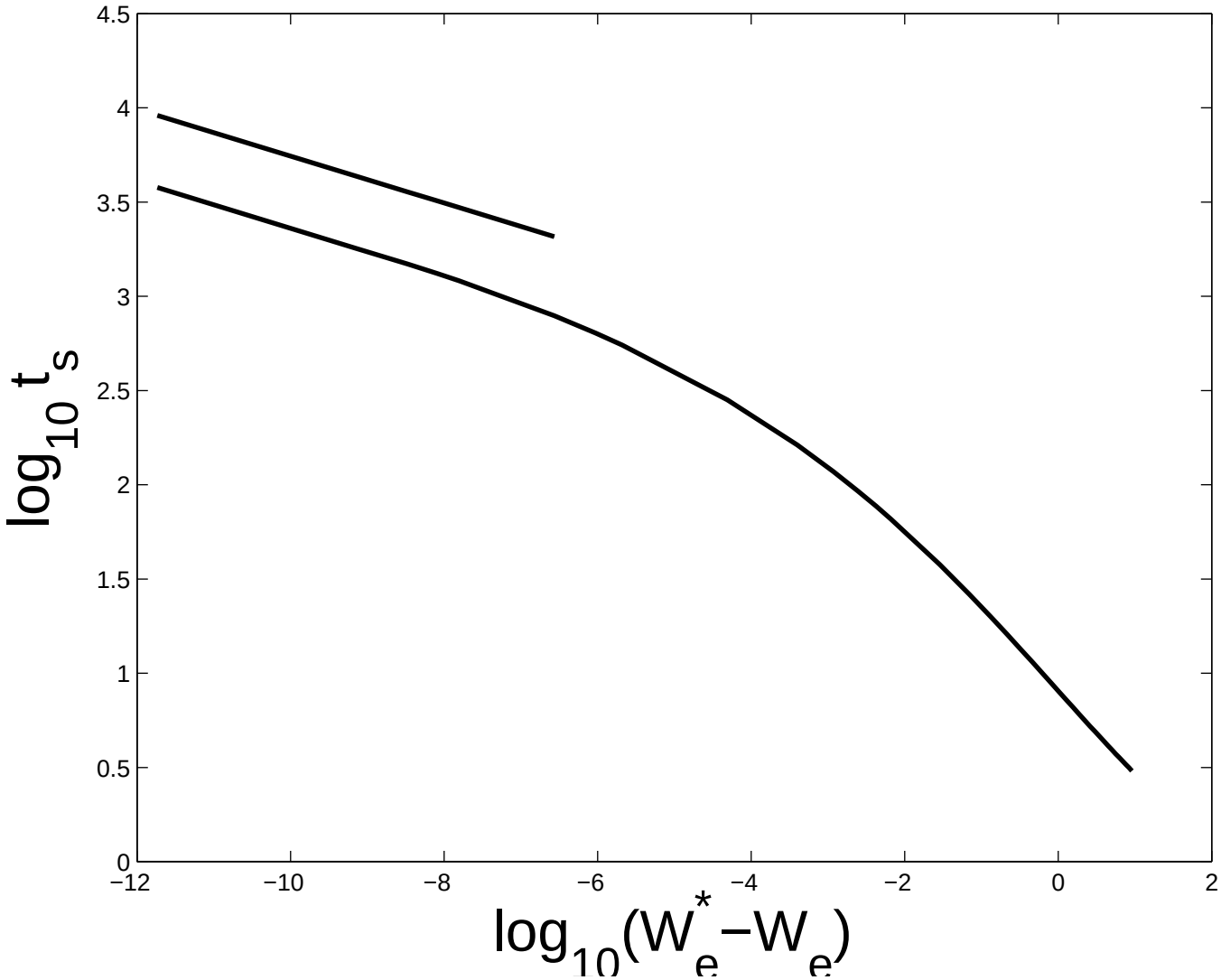

FIG. 5: Savettaseranee, Phys. Fluids

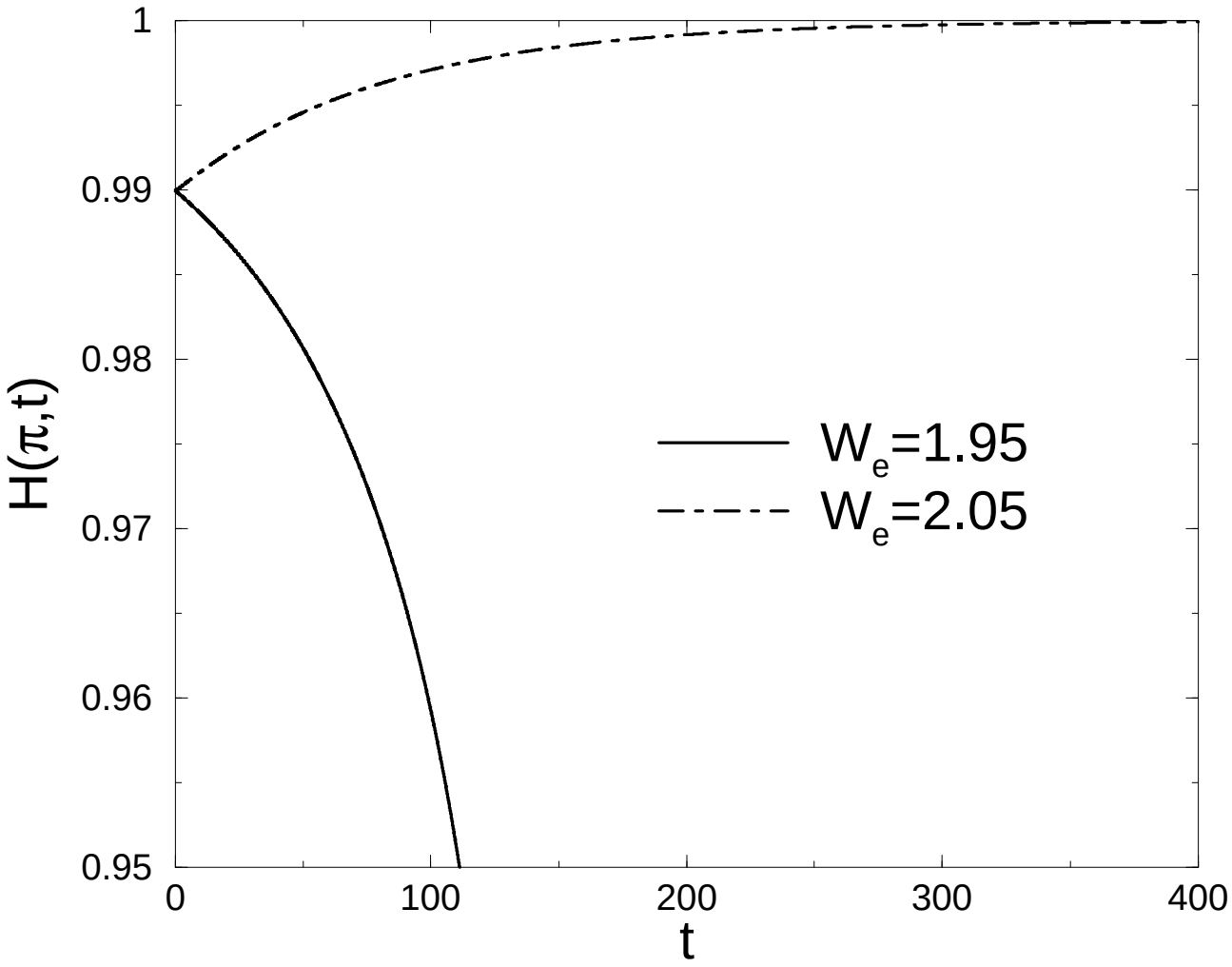

FIG. 6: Savettaseranee, Phys. Fluids

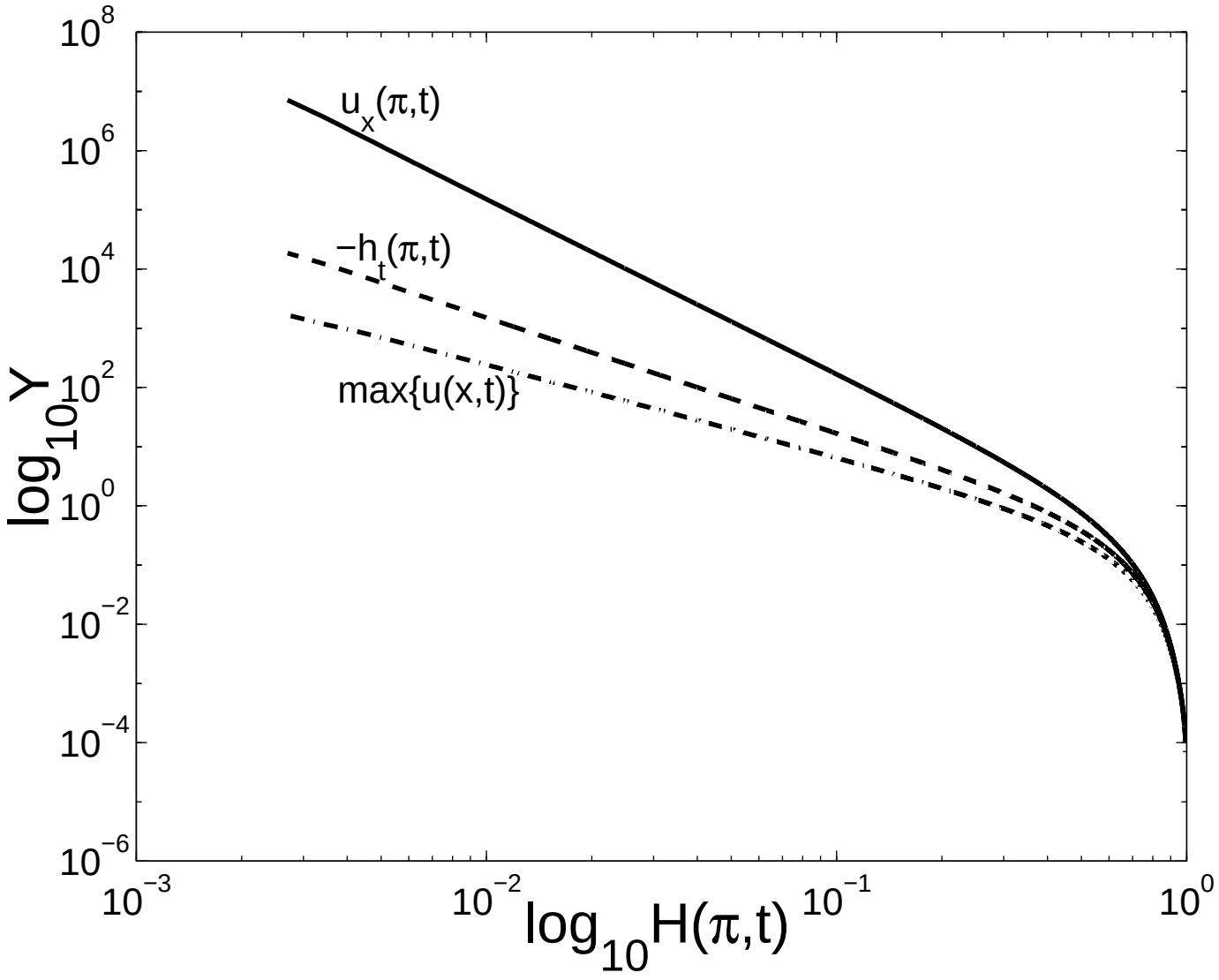

FIG. 7: Savettaseranee, Phys. Fluids

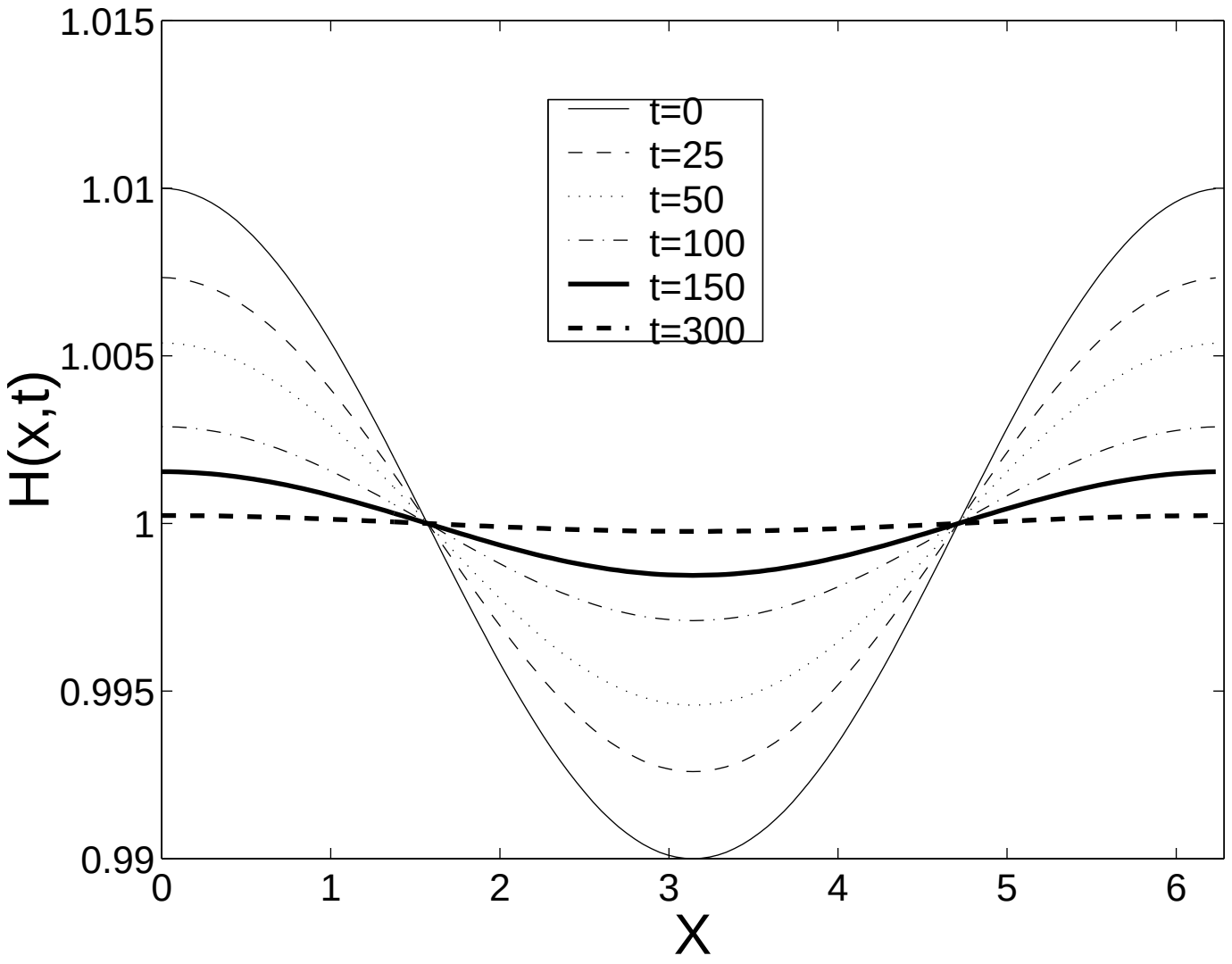

FIG. 8: Savettaseranee, Phys. Fluids